SUPER-RESOLUTION OF REMOTELY SENSED IMAGES USING DRIZZLE AND WAVELETS

Jorge Núñez[1,2] and María Teresa Merino[1]
[1]Departament d'Astronomia i Meteorologia. Universitat de Barcelona, Spain.
[2]Observatori Fabra, Barcelona, Spain.
Te. (+34) 934021129; Fax: (+34) 934021133; jorge@am.ub.es; mmerino@am.ub.es

KEY WORDS: Super-Resolution; Image fusion; Drizzle; Wavelets.

ABSTRACT In this paper, we present the development and application of two algorithms useful for combining a set of undersampled, lower resolution remotely sensed images in a super-resolution product. The first method, called SRVPLR, is based on the Variable-Pixel Linear Reconstruction method (Drizzle) which is a method well known in Astronomy for the combination of undersampled images obtained with the Hubble Space Telescope and other instruments, but has never been used in Remote Sensing for image super-resolution. The second method, called SRASW, is a completely new method based on the image fusion scheme using the multiresolution wavelet decomposition. Both methods preserve photometry, can weight input images according the statistical significance of each pixel, and remove the effect of geometric distortion on both image shape and photometry. We present the development of both methods for Remote Sensing and a first application to: 1) a set of simulated multispectral images of the QuickBird satellite (starting from a real Quickbird image of Madrid) and 2) a set of multispectral real images of Barcelona area obtained by the Landsat ETM+ satellite. The results show that we obtained a high degree of super-resolution (about a factor of 2) for both simulated and real data without altering the multispectral content of the original images or amplifying the noise.

1. INTRODUCTION

In remote sensing, as in many other fields, the spatial resolution of the image is key parameter. Thus, the increment of resolution is a need for many civilian and military applications. One way of obtaining higher resolution images is by increasing the focal length of the satellite-based observing cameras. However, this implies larger, better-stabilized and much more expensive platforms. Another way is to increment the number of pixels of the detectors by reducing its size. This is technically difficult, decrease the amount of collected light by each pixel and increase the shot and readout noise at the detector. Another way to is to apply digital techniques to combine a set of low resolution images (LR) to obtain a super-resolution (HR) result (Park et al., 2003).

A complete super-resolution method should include three steps: 1) Corregister all the LR images of the set; 2) Interpolate and/or combine the LR images over a HR image and 3) Restore the HR image from noise and PSF convolution . The schedule of a super-resolution method is as follows:

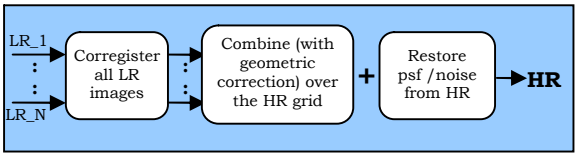

Figure 1: Super-Resolution scheme.

The aim of this paper is to contribute in the second step by the development of two algorithms for the optimal combination of LR undersampled images in a super-resolution result.

2. SRVPLR

Fruchter and Hook (2001) developed the Super-Resolution Variable-Pixel Linear Reconstruction method (SRVPLR or Drizzle) for the linear reconstruction of an image from a set of undersampled, dithered lower resolution images. This method is well known in Astronomy for the combination of undersampled images obtained with the Hubble Space Telescope and other astronomical instruments, but it has never used for Remote Sensing super-resolution. The SRVPLR method preserves photometry, can weight input images according the statistical significance of each pixel, and removes the effect of geometric distortion on both image shape and photometry. The method (see Figure 2) works as follows: once performed the registering process (and histogram matching if needed), obtaining a bi-cubic polynomial, which takes into account translation, rotation and geometric distortion, the method projects, and add each LR image over a HR grid. The key of the method is that during this process, to avoid convolving again the resulting image with the original pixel, the pixels of the LR image are condensed in a "drop" of smaller size. The drops then "rain" over the HR image adding its value to the HR pixels with a weight proportional to the intersecting area between the drop and the HR pixels.

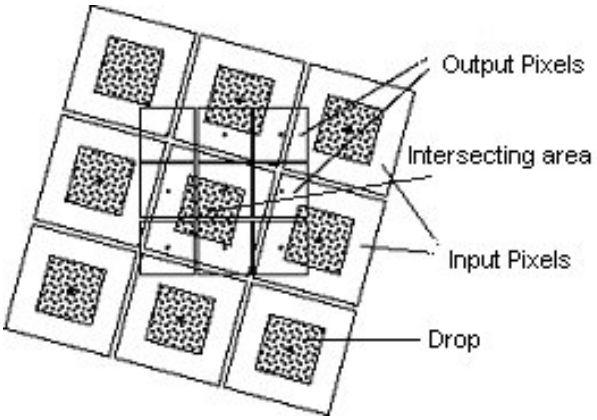

Figure 2: Graphical description of SRVPLR

Analytically, the method works as follows. Let (x_i,y_i) a LR input pixel with value d_{xi1yi1} and user defined weight w_{xi1yi1}. Let (x_o,y_o) an output HR pixel with value I_{xoyo} and weight W_{xoyo}. Let $a_{xiyixoyo}$ (≤ 1) the intersecting area between the condensation drop of (x_i,y_i) and the pixel (x_o,y_o). The resulting intensity of the output pixel I'_{xoyo} and its new weight W'_{xoyo} are:

$$W'_{x_o y_o} = a_{x_i y_i x_o y_o} \cdot w_{x_i y_i} + W_{x_o y_o}$$

$$I'_{x_o y_o} = \frac{d_{x_i y_i} \cdot a_{x_i y_i x_o y_o} \cdot w_{x_i y_i} \cdot s^2 + I_{x_o y_o} W_{x_o y_o}}{W'_{x_o y_o}}$$

where **s** is the scaling factor between HR and LR and is introduced to keep the surface intensity. The relative size of the drop side respect the input pixel is given by parameter **p** (*pixfrac*). After processing all input images, the HR image intensities and weights are:

$$W_{x_o y_o} = \sum_{x_i y_i} a_{x_i y_i x_o y_o} \cdot w_{x_i y_i}$$

$$I_{x_o y_o} = \frac{\sum_{x_i y_i} d_{x_i y_i} \cdot a_{x_i y_i x_o y_o} \cdot w_{x_i y_i} \cdot s^2}{W_{x_o y_o}}$$

where almost all intersecting areas $a_{xiyixoyo}$ are zero because an input pixel affects few output pixels. The algorithm is applied pixel by pixel for all input images to combine giving a HR image which contains the useful information and weight map of all input images.

3. SRASW

The Super Resolution Additive/Substitutive Wavelet-based method (SRASW) is a completely new method based on the image fusion scheme using the multiresolution wavelet decomposition (Núñez et al, 1999a, 1999b). The main idea of the method is: a) Corregister and expand all the LR images to a finer grid. b) Decompose all LR input images in wavelet planes. c) Add over one of the images the first wavelet planes (usually one) of the others. Since the detail information of the image is located in the first wavelet planes, it is fused and included in the resulting image.

In summary, the image wavelet decomposition method is based on the decomposition of the image into multiple channels based on their local frequency content. The wavelet transform provides a framework to decompose images into a number of new images, each one of them with a different degree of resolution. While the Fourier transform gives an idea of the frequency content in our image, the wavelet representation is an intermediate representation between the Fourier and the spatial representation, and it can provide good localization in both frequency and space domains. We skip here details about the wavelet decomposition theory. For more details, see, for example, Daubechies (1992), Núñez et al (1999a) and references therein.

To obtain shift-invariant discrete wavelet decomposition for images, we follow Starck and Murtagh (1994), and use the discrete wavelet transform known as "*à trous*" ("with holes") algorithm to decompose the image into wavelet planes. Given an image **P** we construct the sequence of approximations: $F_1(\mathbf{P}) = \mathbf{P_1}$; $F_2(\mathbf{P_1}) = \mathbf{P_2}$; $F_3(\mathbf{P_2}) = \mathbf{P_3}$ ..... To construct the sequence, this algorithm performs successive convolutions with a filter obtained from an auxiliary function named scaling function. We use a scaling function, which has a $\mathbf{B_3}$ cubic spline profile. The use of a $\mathbf{B_3}$ cubic spline leads to a convolution with a mask of 5x5:

$$\frac{1}{256}\begin{pmatrix} 1 & 4 & 6 & 4 & 1 \\ 4 & 16 & 24 & 16 & 4 \\ 6 & 24 & 36 & 24 & 6 \\ 4 & 16 & 24 & 16 & 4 \\ 1 & 4 & 6 & 4 & 1 \end{pmatrix}$$

The wavelet planes are computed as the differences between two consecutive approximations of the image $\mathbf{P_{m-1}}$ and $\mathbf{P_m}$. Letting $\mathbf{W_m} = \mathbf{P_{m-1}} - \mathbf{P_m}$ (m=1...n) in which $\mathbf{P_0} = \mathbf{P}$ we can write the reconstruction formula:

$$P = \sum_{m=1}^{n} W_m + P_r$$

In this representation, the images $\mathbf{P_m}$ (m=1...n) are versions of the original $\mathbf{P_m}$ at increasing scales (decreasing resolution levels), $\mathbf{W_m}$ (m=1...n) are the multiresolution wavelet planes and $\mathbf{P_r}$ is a residual image, which contains all the energy of the image since the wavelet planes have zero mean. In our case, we are using a dyadic decomposition scheme. Thus, the original image $\mathbf{P_0}$ has double resolution than $\mathbf{P_1}$, the image $\mathbf{P_1}$ double resolution than $\mathbf{P_2}$ and so on. If the resolution of image $\mathbf{P_0}$ is, for example, 10 m, the resolution of $\mathbf{P_1}$ would be 20 m, the resolution of $\mathbf{P_2}$ would be 40m etc. Note, however, that all the consecutive approximations (and wavelet planes) in this process have the same number of pixels as the original image.

The implementation of the SRASW is as follows: 1) Register all LR images (and perform histogram matching if needed) as in previous method obtaining a bi-cubic polynomial for each LR. 2) Expand each LR image to the final HR grid. In this step, we use the SRVPLR method to project each LR image onto an empty grid, using a convenient drop size (pixfrac). 3) Decompose all expanded LR images in wavelet planes as described above. 4) Choose one of the expanded LR

images as reference (usually the same used as reference for the registering process). 5) Add all the detail information contained in the expanded LR images on the reference image. This is performed by substituting the first wavelet plane of the reference image by the mean of the first wavelet plane of all expanded LR. 6) Reconstruct the resulting image using the reconstruction formula. This is the HR result of the SRASW method which contains the energy of the reference image and includes all the combined detail information of all LR images in a finer grid.

4. EXAMPLES

4.1 Simulated Quickbird data

The first example presented is using simulated QuickBird satellite data. We performed such simulation to have a "true" HR image to compare the super-resolution results. To simulate the data we used a real 2.4m pixel RGB multispectral QuickBird image of Madrid. Using this image, we generate 9 simulated RGB images of 4.8m pixelsize. This was performed by rotating the original 2.4m pixel image in steps of 20 degrees and degrading it to the new pixelsize of 4.8m. To minimize neighbor pixel contamination in this step (and simulate a true 4.8m sensor as much as possible) we first expanded the original image, using SRVPLR, to a fine 0.6m pixel grid and then degrade it to 4.8m by integrating the finer pixels. We applied SRVPLR and SRASW to combine the 9 4.8m pixel images in a 2.4m pixel Super-Resolution result. Figure 3 shows the results.

Figure 3: Results of appling SRVPLR and SRASW to a set of simulated QuickBird images. From left to right: **a)** One of the 9 input 4.8m pixel LR images. **b)** SRVPLR 2.4m pixel result. **c)** SRASW 2.4m pixel result and **d)** Original 2.4m true image.

Figure 3 show the high degree of Super-resolution obtained using both methods. Although it is not possible to recover the 2.4m resolution of the original image, the results show a obtained resolution much closer to the 2.4m original than to the 4.8m of the input images. Also, both methods preserve very well the multispectral characteristics of the original image with correlations of 0.99 in each R,G,B bands between the results and the original image.

4.2 Real Landsat ETM+ data

For the second example, we used 9 real RGB multispectral Landsat ETM+ images of Barcelona. The 30m pixel RGB images were obtained along 2 years at different epoch of the year. Thus, Seasonal and temporal effects are high. We register the images using 60 control points and applied SRVPLR and SRASW to combine the nine 30m pixel RGB images in a 15m pixel Super-Resolution RGB result. Since in this case we do not have an original image, we use the 15m PAN image of one of them to check the obtained super-resolution degree. Figure 4 shows the results.

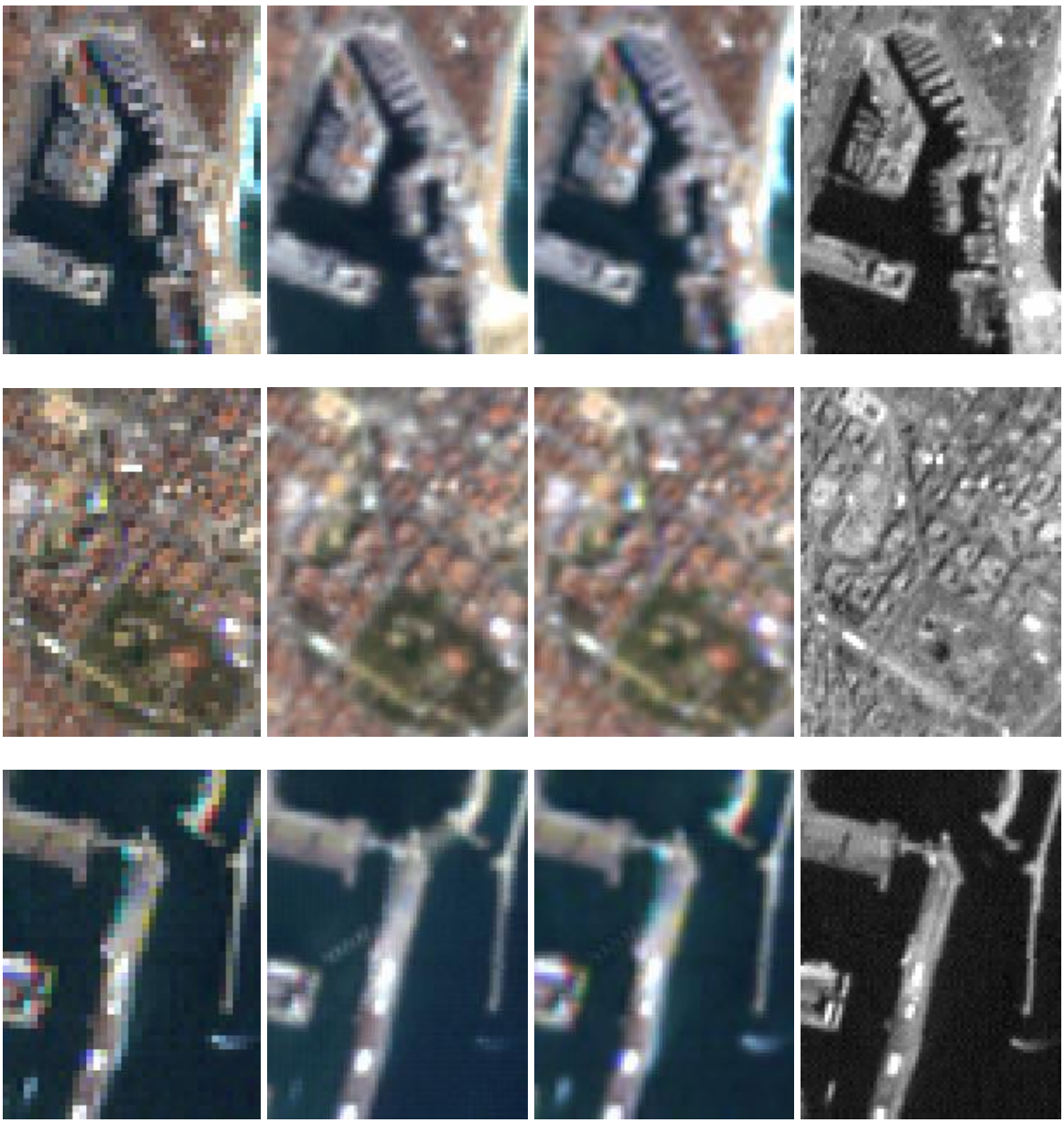

Figure 4: Results of appling SRVPLR and SRASW to a set of 9 real Landsat ETM+ images. From left to right: **a)** One of the 9 input 30m pixel LR images. **b)** SRVPLR 15m pixel result. **c)** SRASW 15m pixel result and **d)** PAN image of 15m pixel corresponding to the left image.

Again, Figure 4 show the high degree of Super-resolution obtained using both methods. The recovered details of the harbor or of the streets show that we obtained a resolution closer to the 15m PAN image than to the 30m of the input images while preserving very well the multispectral characteristics of the input RGB images. In fact, since the SRVPLR and SRASW results are multispectral, in is possible to see in the resulting images in some places more detail than in the 15m Panchromatic image. This is particularly remarkable taking into account that, as mentioned, the input images suffer of seasonal and strong temporal effects.

5. CONCLUSIONS

We have designed, and applied to Remote Sensing, two new algorithms to obtain Super-Resolution by combining a set of undersampled low resolution images. One of the algorithms, the Variable-Pixel Linear Reconstruction method (SRVPLR), is common in astronomical image processing but never applied in Remote Sensing for image super-resolution. The second method, (SRASW), is a completely new method based on the multiresolution wavelet decomposition image fusion. Both methods remove the effect of geometric distortion, preserve photometry and weight input images according the statistical significance. To check the methods, we applied them to both simulated and real multispectral images of the QuickBird and Landsat ETM+ satellites. The results show that we obtained almost a factor of 2 of super-resolution for both simulated and real data without amplifying the noise or altering the multispectral content of the original images. This was true even in the case of the real Landsat images severely affected by seasonal and temporal effects.

6. ACKNOWLEDGEMENTS

The images used in this work were facilitated by The Institito Nacional de Técnica Aeroespacial (INTA) and by the Departament de Geografia of the Universitat Autònoma de Barcelona.

7. REFERENCES

Daubechies, I., 1992. Ten lectures on wavelets. SIAM Press, Philadelphia.

Fruchter, A.S., Hook, R.N., 2001. Drizzle: a method for linear reconstruction of undersampled images. Publ. Aastron. Soc. Pacific, 114, pp.144-152.

Núñez, J., Otazu, X., Fors, O., Palà, V., Arbiol, R., 1999a. Multiresolution-based image fusion with additive wavelet decomposition. IEEE Trans. on Geosc. and Remote Sensing, 37, n. 3, pp.1204-1211.

Núñez, J., Otazu, X., Fors, O., Palà, V., Arbiol, R., 1999b, Image fusion using additive multiresolution wavelet decomposition. Applications to SPOT + LANDSAT images. Journal of the Optical Soc. Amer., ser. A, 16, n. 3, pp. 467-474.

Park, S.C., Park, M.K., Kang, M.G., 2003. Super-Resolution image reconstruction: A technical overview. IEEE Signal Processing Magazine, 20, n.3, pp. 21-36.

Starck, J.L., Murtagh, F., 1994. Image restoration with noise suppression using the wavelet transform. Astronomy and Astrophysics, 288, pp.342-350.